W boson mass in gauge-Higgs unification

Yutaka Hosotani,[1,*] Shuichiro Funatsu,[2] Hisaki Hatanaka,[3] Yuta Orikasa,[4] and Naoki Yamatsu[5]

[1]*Research Center for Nuclear Physics, Osaka University, Ibaraki, Osaka 567-0047, Japan*
[2]*Ushiku, Ibaraki 300-1234, Japan*
[3]*Osaka, Osaka 536-0014, Japan*
[4]*Institute of Experimental and Applied Physics, Czech Technical University in Prague, Husova 240/5, 110 00 Prague 1, Czech Republic*
[5]*Department of Physics, National Taiwan University, Taipei, Taiwan 10617, Republic of China*

(Received 6 October 2023; accepted 1 December 2023; published 27 December 2023)

The W boson mass m_W in the grand unified theory inspired $SO(5) \times U(1) \times SU(3)$ gauge-Higgs unification in the Randall-Sundrum (RS) warped space is evaluated. The muon decay $\mu^- \to e^- \bar{\nu}_e \nu_\mu$ proceeds by the exchange of not only the zero mode of the W boson $(W^{(0)})$ but also Kaluza-Klein (KK) excited modes $W^{(n)}$ and $W_R^{(n)}$ $(n \geq 1)$ at the tree level. The anti–de Sitter curvature of the RS space also affects the relationship among the gauge couplings and the ratio of m_W to the Z boson mass m_Z. The W couplings of leptons and quarks also change. With the given KK mass scale $m_{\rm KK}$ the range of the Aharonov-Bohm phase θ_H in the fifth dimension is constrained. For $m_{\rm KK} = 13$ TeV, $0.085 \lesssim \theta_H \lesssim 0.11$ and $80.381 \lesssim m_W \lesssim 80.407$ GeV. The predicted value of m_W for $13 \leq m_{\rm KK} \leq 20$ TeV lies between $m_W^{\rm SM} = 80.354 \pm 0.007$ GeV in the standard model and $m_W^{\rm CDF} = 80.4335 \pm 0.0094$ GeV, the value reported by the CDF Collaboration in 2022.

DOI: 10.1103/PhysRevD.108.115036

I. INTRODUCTION

Last year, the CDF Collaboration reported on the mass of the W boson, $m_W^{\rm CDF} = 80.4335 \pm 0.0094$ GeV [1]. The predicted value in the standard model (SM) is $m_W^{\rm SM} = 80.354 \pm 0.007$ GeV [2–4]. The discrepancy between the two has triggered huge debates on possible new physics beyond the SM. The ATLAS Collaboration also reanalyzed the data in 2011 to obtain $m_W^{\rm ATLAS} = 80.360 \pm 0.016$ GeV [5]. Although the experimental situation has not been settled yet, it is worth examining various models to find whether or not they can lead to a larger value for m_W than $m_W^{\rm SM}$ without conflicting with other observations at low energies.

There have been various proposals to account for the m_W anomaly. Many of them are based on new physics effects on the Peskin-Takeuchi oblique S and T parameters [6–10], either at the tree level [11,12] or at the loop level [13–15]. Another approach is based on a scenario in which new fields and/or couplings give additional contributions to the Fermi constant G_F [16,17].

It has been known that the SM $SU(3)_C \times SU(2)_L \times U(1)_Y$ gauge theory, though being mostly successful in describing phenomena at low energies, has a severe gauge hierarchy problem when embedded in a larger theory such as grand unification. As one possible answer to this problem, the gauge-Higgs unification (GHU) scenario has been proposed in which gauge symmetry is dynamically broken by an Aharonov-Bohm (AB) phase θ_H in the fifth dimension. The 4D Higgs boson appears as a 4D fluctuation mode of θ_H [18–34].

Among various GHU models, the $SO(5) \times U(1) \times SU(3)$ GHU in the Randall-Sundrum (RS) warped space, inspired from the $SO(11)$ gauge-Higgs grand unification model [35], has been extensively investigated [32–34]. It has been shown that the grand unified theory (GUT) inspired GHU yields nearly the same phenomenology at low energies as the SM. GHU models in the RS warped space predict, in general, large parity violation in the couplings of quarks and leptons to Kaluza-Klein (KK) excited modes of gauge bosons, which can be clearly seen, for $m_{\rm KK} \sim 13$ TeV, for instance, at electron-positron $(e^- e^+)$ colliders such as ILC with $\sqrt{s} = 250$ GeV by using polarized e^- and e^+ beams [36–40]. Deviation from the SM can be explored also in the processes of $W^- W^+$ production and single Higgs production in $e^- e^+$ collisions [41,42]. Signals of Z' particles, namely, KK excited modes of γ, Z, and Z_R gauge bosons, should be seen in high-luminosity LHC as well [43].

*hosotani@rcnp.osaka-u.ac.jp

KK modes of fermions and gauge bosons in the RS warped space have quite nontrivial couplings. Recently, oblique corrections to γ, Z, and W propagators at the one loop level in the GUT inspired GHU have been evaluated [44]. Inside the loops, all possible KK modes of fermions run. The total oblique corrections to S, T, and U turned out to be small as a consequence of the coupling sum rules, special relations holding among infinitely many gauge couplings in the KK mode space. In the GHU scenario the 5D gauge invariance seems to lead to many surprising coupling relations among zero modes and KK excited modes of fermions and gauge bosons. It has been shown in the $SU(2)$ GHU model in the RS space that gauge anomalies associated with various 4D modes of gauge fields vary with the AB phase θ_H. The total gauge anomalies obtained by summing contributions from all fermion KK modes are expressed in terms of the values of the gauge field wave functions at the UV and IR branes of the RS space, representing relations among gauge couplings of right- and left-handed fermions [45,46].

In view of these facts, one may ask how large the W boson mass m_W is in the GUT inspired GHU. There are KK excited modes of W and W_R gauge bosons that couple to leptons and contribute to the muon decay at the tree level. Further, the relation between the gauge couplings and the ratio of the W and Z boson masses m_W/m_Z is changed even at the tree level. In this paper, we analyze this matter in detail. Additional relevant parameters in the GUT inspired GHU are the KK mass scale $m_{\rm KK}$ and the AB phase θ_H. It will be seen below that, for $m_{\rm KK} = 13$ TeV, for instance, $0.085 \lesssim \theta_H \lesssim 0.11$ is allowed and m_W becomes $80.381 \lesssim m_W \lesssim 80.407$ GeV. The dominant contributions come from large gauge couplings of left-handed leptons to the first KK excited mode of the W boson $W^{(1)}$, the change in the W couplings of leptons (e and μ), and the change in the relation between the gauge couplings and mass ratio m_W/m_Z in the RS warped space.

In Sec. II the GUT inspired $SO(5) \times U(1)_X \times SU(3)_C$ GHU model is explained. In Sec. III the W boson mass is evaluated. It will be seen that the predicted value of m_W in the GUT inspired GHU is mostly determined by the value of θ_H. A summary is given in Sec. IV.

II. GUT INSPIRED GHU

The GUT inspired $SO(5) \times U(1)_X \times SU(3)_C$ GHU was introduced in Ref. [32]. It is defined in the RS warped space, whose metric is given by [47]

$$ds^2 = g_{MN}dx^M dx^N = e^{-2\sigma(y)}\eta_{\mu\nu}dx^\mu dx^\nu + dy^2, \quad (2.1)$$

where $M,N = 0,1,2,3,5$, $\mu,\nu = 0,1,2,3$, $y = x^5$, $\eta_{\mu\nu} = \mathrm{diag}(-1,+1,+1,+1)$, $\sigma(y) = \sigma(y+2L) = \sigma(-y)$, and $\sigma(y) = ky$ for $0 \le y \le L$. In terms of the conformal coordinate $z = e^{ky}$ ($0 \le y \le L$, $1 \le z \le z_L = e^{kL}$),

$$ds^2 = \frac{1}{z^2}\left(\eta_{\mu\nu}dx^\mu dx^\nu + \frac{dz^2}{k^2}\right). \quad (2.2)$$

The bulk region $0 < y < L$ is anti–de Sitter (AdS) spacetime with a cosmological constant $\Lambda = -6k^2$, which is sandwiched by the UV brane at $y = 0$ and the IR brane at $y = L$. z_L is called as the warp factor. The KK mass scale is given by $m_{\rm KK} = \pi k/(z_L - 1) \simeq \pi k z_L^{-1}$ for $z_L \gg 1$.

Gauge fields $A_M^{SO(5)}$, $A_M^{U(1)_X}$, and $A_M^{SU(3)_C}$ of $SO(5) \times U(1)_X \times SU(3)_C$ satisfy the orbifold boundary conditions (BCs)

$$\begin{pmatrix} A_\mu \\ A_y \end{pmatrix}(x, y_j - y) = P_j \begin{pmatrix} A_\mu \\ -A_y \end{pmatrix}(x, y_j + y) P_j^{-1} \quad (j = 0,1), \quad (2.3)$$

where $(y_0, y_1) = (0, L)$. Here $P_0 = P_1 = P_{\mathbf{5}}^{SO(5)} = \mathrm{diag}(I_4, -I_1)$ for $A_M^{SO(5)}$ in the vector representation and $P_0 = P_1 = 1$ for $A_M^{U(1)_X}$ and $A_M^{SU(3)_C}$. The 4D Higgs field is contained in the $SO(5)/SO(4)$ part of $A_y^{SO(5)}$. The orbifold BCs break $SO(5)$ to $SO(4) \simeq SU(2)_L \times SU(2)_R$.

The matter content in the GUT inspired GHU is summarized in Table I. Quark and lepton multiplets are introduced in three generations. The lepton multiplets $\Psi^\alpha_{(\mathbf{1},\mathbf{4})}(x,y)$ ($\alpha = 1,2,3$) satisfy BCs

$$\Psi^\alpha_{(\mathbf{1},\mathbf{4})}(x, y_j - y) = -P_{\mathbf{4}}^{SO(5)} \gamma^5 \Psi^\alpha_{(\mathbf{1},\mathbf{4})}(x, y_j + y), \quad (2.4)$$

where $P_{\mathbf{4}}^{SO(5)} = \mathrm{diag}(I_2, -I_2)$. (For BCs of other multiplets, see Refs. [32] or [44].) The action of $\Psi^\alpha_{(\mathbf{1},\mathbf{4})}$ in the bulk is

$$\begin{aligned} S_{\rm bulk}^{\rm lepton} &= \int d^5x \sqrt{-\det G} \sum_\alpha \bar\Psi^\alpha_{(\mathbf{1},\mathbf{4})} \mathcal{D}(c_\alpha) \Psi^\alpha_{(\mathbf{1},\mathbf{4})}, \\ \mathcal{D}(c) &= \gamma^A e_A{}^M \left(D_M + \frac{1}{8}\omega_{MBC}\left[\gamma^B, \gamma^C\right]\right) - c\sigma'(y), \\ D_M &= \partial_M - i g_A A_M^{SO(5)} - i g_B Q_X A_M^{U(1)}. \end{aligned} \quad (2.5)$$

TABLE I. The matter fields in the GUT inspired $SO(5) \times U(1) \times SU(3)$ gauge-Higgs unification. $(SU(3)_C, SO(5))_{U(1)_X}$ content of each field is shown in the last column.

In the bulk	Quark	$(\mathbf{3},\mathbf{4})_{\frac{1}{6}}(\mathbf{3},\mathbf{1})^+_{\frac{1}{3}}(\mathbf{3},\mathbf{1})^-_{-\frac{1}{3}}$
	Lepton	$(\mathbf{1},\mathbf{4})_{-\frac{1}{2}}$
	Dark fermion Ψ^D	$(\mathbf{3},\mathbf{4})_{\frac{1}{6}}(\mathbf{1},\mathbf{5})^+_0(\mathbf{1},\mathbf{5})^-_0$
On the UV brane	Majorana fermion χ	$(\mathbf{1},\mathbf{1})_0$
	Brane scalar Φ	$(\mathbf{1},\mathbf{4})_{\frac{1}{2}}$

The dimensionless parameter c in $\mathcal{D}(c)$ is called the bulk mass parameter, which controls the wave functions of the zero modes of the fermions. In the GUT inspired GHU, the bulk mass parameters are negative for both lepton and quark multiplets. On the UV brane at $y = 0$, gauge-singlet Majorana fermions $\chi^{\alpha}_{(\mathbf{1},\mathbf{1})}$ and one brane scalar $\Phi_{(\mathbf{1},\mathbf{4})}$ are introduced. There arise gauge-invariant brane interactions of the form $\{\tilde{\kappa}^{\alpha\beta}_{\mathbf{1}}\bar{\chi}^{\beta}_{(\mathbf{1},\mathbf{1})}\tilde{\Phi}^{\dagger}_{(\mathbf{1},\mathbf{4})}\Psi^{\alpha}_{(\mathbf{1},\mathbf{4})} + \text{H.c.}\}\delta(y)$, where $\tilde{\Phi}_{(\mathbf{1},\mathbf{4})}$ denotes a conjugate field in $(\mathbf{1},\mathbf{4})$ formed from $\Phi^{*}_{(\mathbf{1},\mathbf{4})}$. The brane scalar field $\Phi_{(\mathbf{1},\mathbf{4})}$ spontaneously develops a nonvanishing expectation value $\langle\Phi\rangle \neq 0$, which, with the brane interaction term, induces the inverse seesaw mechanism for neutrinos.

In the electroweak sector, there are two 5D gauge couplings, g_A and g_B, corresponding to the gauge groups $SO(5)$ and $U(1)_X$, respectively. The 5D gauge coupling g_Y^{5D} of $U(1)_Y$ is given by $g_Y^{5D} = g_A g_B/\sqrt{g_A^2 + g_B^2}$. The 4D $SU(2)_L$ and $U(1)_Y$ gauge coupling constants are given by $g_w = g_A/\sqrt{L}$ and $g_Y = g_Y^{5D}/\sqrt{L}$. The bare weak mixing angle $\bar{\theta}_W^0$ determined by the ratio of the gauge couplings is given by

$$\sin\bar{\theta}_W^0 = \frac{g_Y}{\sqrt{g_w^2 + g_Y^2}} = \frac{g_B}{\sqrt{g_A^2 + 2g_B^2}}. \tag{2.6}$$

As is seen below, the mixing angle determined from the ratio m_W/m_Z slightly differs from the one defined in (2.6) even at the tree level in GHU in the RS space.

The 4D Higgs boson field $\Phi_H(x)$ appears as a part of $A_y^{SO(5)}$. $A_z^{SO(5)} = (kz)^{-1}A_y^{SO(5)}$ $(1 \le z \le z_L)$ in the tensor representation is expanded as

$$A_z^{(j5)}(x,z) = \frac{1}{\sqrt{k}}\phi_j(x)u_H(z) + \cdots, \qquad u_H(z) = \sqrt{\frac{2}{z_L^2 - 1}}z,$$
$$\Phi_H(x) = \frac{1}{\sqrt{2}}\begin{pmatrix}\phi_2 + i\phi_1 \\ \phi_4 - i\phi_3\end{pmatrix}. \tag{2.7}$$

Φ_H develops nonvanishing expectation value at the quantum level by the Hosotani mechanism. Without loss of generality, we take $\langle\phi_1\rangle, \langle\phi_2\rangle, \langle\phi_3\rangle = 0$ and $\langle\phi_4\rangle \neq 0$. The AB phase θ_H in the fifth dimension is given by

$$\hat{W} = P\exp\left\{ig_A\int_{-L}^{L}dy\langle A_y^{SO(5)}\rangle\right\} = \exp\{i\theta_H\cdot 2T^{(45)}\}. \tag{2.8}$$

In terms of θ_H, $A_z^{(45)}$ is expanded as

$$A_z^{(45)}(x,z) = \frac{1}{\sqrt{k}}\{\theta_H f_H + H(x)\}u_H(z) + \cdots,$$
$$f_H = \frac{2}{g_A}\sqrt{\frac{k}{z_L^2 - 1}} = \frac{2}{g_w}\sqrt{\frac{k}{L(z_L^2 - 1)}}. \tag{2.9}$$

The 4D neutral Higgs field $H(x)$ is the fluctuation mode of the AB phase θ_H.

The AB phase θ_H plays an important role in GHU. The value of θ_H is determined by the location of the absolute minimum of the effective potential $V_{\text{eff}}(\theta_H)$, and the Higgs boson mass m_H is given by $m_H^2 = f_H^{-2}d^2V_{\text{eff}}(\theta_H)/d\theta_H^2|_{\text{min}}$. With the KK mass scale m_{KK} given, the allowed range of θ_H is constrained to reproduce the Higgs boson and top quark masses and also to be consistent with the current observations at low energies.

III. THE W BOSON MASS

In the SM, the Fermi constant G_μ determined from the μ decay is given by [48]

$$\frac{G_\mu}{\sqrt{2}} = \frac{\pi\alpha}{2s_W^2}\frac{1}{m_W^2}(1 + \Delta r_{\text{SM}}^{\text{loop}}), \tag{3.1}$$

$$s_W^2 = 1 - \frac{m_W^2}{m_Z^2}, \tag{3.2}$$

where $\alpha^{-1} = 137.035999084(21)$, $G_\mu = 1.1663788(6)\times 10^{-5}$ GeV^{-2}, and $m_Z = 91.1876(21)$ GeV [49]. $\Delta r_{\text{SM}}^{\text{loop}}$ represents the sum of all loop corrections, which depends on α, m_W, m_Z, m_H, strong gauge coupling constant, and masses of quarks and leptons. Combining Eqs. (3.1) and (3.2), one can write the W boson mass in the SM as

$$m_W^{\text{SM}} = \frac{m_Z}{\sqrt{2}}\left[1 + \sqrt{1 - \frac{4\pi\alpha(1 + \Delta r_{\text{SM}}^{\text{loop}})}{\sqrt{2}G_\mu m_Z^2}}\right]^{1/2}. \tag{3.3}$$

At the tree level, $\Delta r_{\text{SM}}^{\text{loop}} = 0$ so that $m_W^{\text{SM}}|_{\text{tree}} = 80.9387$ GeV, which is much larger than the observed W mass. Significant efforts have been made to evaluate $\Delta r_{\text{SM}}^{\text{loop}}$. At the moment, the estimated value is $\Delta r_{\text{SM}}^{\text{loop}} \simeq 0.0383 \pm 0.0004$ and $m_W^{\text{SM}} \simeq 80.354 \pm 0.007$ GeV [2–4].

In GHU both of the relations (3.1) and (3.2) are modified, even at the tree level. With given θ_H the masses of W and Z, $m_W = k\lambda_W$ and $m_Z = k\lambda_Z$, satisfy [32]

$$2S(1;\lambda_W,z_L)C'(1;\lambda_W,z_L) + \lambda_W\sin^2\theta_H = 0, \tag{3.4}$$

$$2S(1;\lambda_Z,z_L)C'(1;\lambda_Z,z_L) + \frac{\lambda_Z\sin^2\theta_H}{1 - \sin^2\theta_W^0} = 0, \tag{3.5}$$

where the functions $C(z;\lambda,z_L)$ and $S(z;\lambda,z_L)$ are expressed in terms of Bessel functions, as given in Eq. (A1). At the tree level, $\sin^2\theta_W^0$ in (3.5) is equal to $\sin^2\bar{\theta}_W^0$ given in (2.6). With the orbifold boundary condition (2.3), physical m_W and m_Z, and $\sin^2\theta_W^0$ specified, the wave functions of W and Z are determined with the conditions (3.4) and (3.5). The boundary condition does

not change by radiative corrections. In other words, $\sin^2\theta_W^0$ appearing in (3.5) is the bare weak mixing angle in the on-shell scheme in GHU, corresponding to s_W^2 (3.2) in the SM. m_Z is one of the input parameters. With $m_{\rm KK} = \pi k/(z_L - 1)$ specified, the relation (3.5) fixes the value of z_L and k. Then the relation (3.4) determines λ_W and m_W. The ratio m_W/m_Z thus determined is slightly different from $\cos\theta_W^0$. For $\theta_H = 0.1$, $m_{\rm KK} = 13$ TeV, $\sin^2\theta_W^0 = 0.2227$, for instance, one finds $m_W - m_Z\cos\theta_W^0 = -1.59$ MeV.

The value of $\sin^2\theta_W^0$ needs to be determined self-consistently such that the observed G_μ is reproduced. In the GUT inspired GHU α, G_μ, m_Z, strong gauge coupling constant, masses of quarks and leptons, and m_H are input parameters. With given $\sin^2\theta_W^0$, θ_H, and $m_{\rm KK}$, one can evaluate the mass spectra of KK gauge bosons and their couplings to leptons. The μ decay proceeds, at the tree level, by emitting not only $W = W^{(0)}$, but also $W^{(n)}$ and $W_R^{(n)}$ $(n \geq 1)$. Here $W_R^{(n)}$ are gauge bosons in $SU(2)_R$ of $SO(4) = SU(2)_L \times SU(2)_R \subset SO(5)$; hence the relation (3.1) is replaced by

$$\frac{G_\mu}{\sqrt{2}} = \frac{\pi\alpha}{2\sin^2\theta_W^0}\frac{\hat{g}^{W^{(0)}}_{\mu\nu_\mu,L}\hat{g}^{W^{(0)}}_{e\nu_e,L}}{m^2_{W^{(0)}}}(1+\Delta r_G)(1+\Delta r^{\rm loop}_{\rm GHU}),$$

$$\Delta r_G = \frac{1}{\hat{g}^{W^{(0)}}_{\mu\nu_\mu,L}\hat{g}^{W^{(0)}}_{e\nu_e,L}}\sum_{n=1}^{\infty}\left\{\hat{g}^{W^{(n)}}_{\mu\nu_\mu,L}\hat{g}^{W^{(n)}}_{e\nu_e,L}\left[\frac{m_{W^{(0)}}}{m_{W^{(n)}}}\right]^2 + \hat{g}^{W_R^{(n)}}_{\mu\nu_\mu,L}\hat{g}^{W_R^{(n)}}_{e\nu_e,L}\left[\frac{m_{W^{(0)}}}{m_{W_R^{(n)}}}\right]^2\right\}, \tag{3.6}$$

where the coupling of $W^{(n)}$ to $e\nu_e$, for instance, is given by $(g_w/\sqrt{2})W_\mu^{(n)}\{\hat{g}^{W^{(n)}}_{e\nu_e,L}\bar{\nu}_{e,L}\gamma^\mu e_L + \hat{g}^{W^{(n)}}_{e\nu_e,R}\bar{\nu}_{e,R}\gamma^\mu e_R\}$. The right-handed couplings are very small ($|\hat{g}^{W^{(n)}}_{e\nu_e,R}| < 10^{-19}$, etc.) and have been omitted in the expression for Δr_G in (3.6). $\Delta r^{\rm loop}_{\rm GHU}$ represents the sum of loop corrections. In GHU the W boson mass $m_W = m_{W^{(0)}}$ is determined by solving (3.4) and (3.6) simultaneously.

The mass spectra $\{m_{W^{(n)}} = k\lambda_{W^{(n)}}\}$ and $\{m_{W_R^{(n)}} = k\lambda_{W_R^{(n)}}\}$ are determined by

$$2S(1;\lambda_{W^{(n)}},z_L)C'(1;\lambda_{W^{(n)}},z_L) + \lambda_{W^{(n)}}\sin^2\theta_H = 0, \tag{3.7}$$

$$C(1;\lambda_{W_R^{(n)}},z_L) = 0, \tag{3.8}$$

respectively. Wave functions of gauge and fermion fields are also determined, with which gauge couplings among them are evaluated (see [44,50] for details). The values of $\{m_{W^{(n)}}, \hat{g}^{W^{(n)}}_{e\nu_e,L}, \hat{g}^{W^{(n)}}_{\mu\nu_\mu,L}\}$ and $\{m_{W_R^{(n)}}, \hat{g}^{W_R^{(n)}}_{e\nu_e,L}, \hat{g}^{W_R^{(n)}}_{\mu\nu_\mu,L}\}$ are tabulated in Tables II and III for $m_{\rm KK} = 13$ TeV and $\theta_H = 0.10$, respectively. One sees that the $W^{(1)}$ mode has large couplings $\hat{g}^{W^{(1)}}_{e\nu_e,L} \sim 5.721$ and $\hat{g}^{W^{(1)}}_{\mu\nu_\mu,L} \sim 5.446$, giving an appreciable correction to G_μ. The infinite sum in Δr_G in (3.6) is seen to rapidly converge.

TABLE II. The masses $m_{W^{(n)}}$ and couplings $\hat{g}^{W^{(n)}}_{e\nu_e,L}$, $\hat{g}^{W^{(n)}}_{\mu\nu_\mu,L}$ $(n = 0,1,\ldots,9)$ are shown for $m_{\rm KK} = 13$ TeV and $\theta_H = 0.10$ with $\sin^2\theta_W^0 = 0.22266$. Right-handed couplings are very small; $|\hat{g}^{W^{(n)}}_{e\nu_e,R}| < 2\times10^{-20}$ and $|\hat{g}^{W^{(n)}}_{\mu\nu_\mu,R}| < 8\times10^{-19}$ for $n \leq 14$.

n	$m_{W^{(n)}}$(GeV)	$\frac{m_{W^{(n)}}}{m_{\rm KK}}$	$\frac{m_{W^{(0)}}}{m_{W^{(n)}}}$	$\hat{g}^{W^{(n)}}_{e\nu_e,L}$	$\hat{g}^{W^{(n)}}_{\mu\nu_\mu,L}$
0	80.396	0.0062	1	0.997649	0.997646
1	10199	0.7845	7.88×10^{-3}	5.72126	5.44645
2	15857	1.2198	5.07×10^{-3}	0.01858	0.01641
3	23102	1.7771	3.48×10^{-3}	2.26066	1.72755
4	29032	2.2332	2.77×10^{-3}	0.00607	0.00421
5	36074	2.7749	2.23×10^{-3}	0.82175	0.59526
6	42099	3.2384	1.91×10^{-3}	0.00291	0.00226
7	49062	3.7740	1.64×10^{-3}	0.48331	0.36385
8	55135	4.2412	1.46×10^{-3}	0.00173	0.00123
9	62056	4.7735	1.30×10^{-3}	0.28815	0.20853

TABLE III. The masses $m_{W_R^{(n)}}$ and couplings $\hat{g}^{W_R^{(n)}}_{e\nu_e,L}$, $\hat{g}^{W_R^{(n)}}_{\mu\nu_\mu,L}$ $(n = 1,2,\ldots,5)$ are shown for $m_{\rm KK} = 13$ TeV and $\theta_H = 0.10$ with $\sin^2\theta_W^0 = 0.22266$. Right-handed couplings are very small; $|\hat{g}^{W_R^{(n)}}_{e\nu_e,R}| < 2\times10^{-19}$ and $|\hat{g}^{W_R^{(n)}}_{\mu\nu_\mu,R}| < 2\times10^{-17}$ for $n \leq 8$.

n	$m_{W_R^{(n)}}$(GeV)	$\frac{m_{W_R^{(n)}}}{m_{\rm KK}}$	$\frac{m_{W^{(0)}}}{m_{W_R^{(n)}}}$	$\hat{g}^{W_R^{(n)}}_{e\nu_e,L}$	$\hat{g}^{W_R^{(n)}}_{\mu\nu_\mu,L}$
1	9951	0.7655	8.08×10^{-3}	0.01449	0.01382
2	22842	1.7571	3.52×10^{-3}	0.00579	0.00445
3	35809	2.7546	2.25×10^{-3}	0.00209	0.00151
4	48794	3.7534	1.65×10^{-3}	0.00122	0.00092
5	61785	4.7527	1.30×10^{-3}	0.00073	0.00053

$\Delta r^{\rm loop}_{\rm GHU}$ in (3.6) represents radiative corrections. KK excited modes of gauge bosons, leptons, and quarks give little contribution to $\Delta r^{\rm loop}_{\rm GHU}$, as their masses are of $O(m_{\rm KK})$ and $m_\mu/m_{\rm KK} \ll 1$. Only SM particles give relevant contributions to $\Delta r^{\rm loop}_{\rm GHU}$, and the couplings among the SM particles are nearly the same as in the SM (for instance, $\hat{g}^{W^{(0)}}_{e\nu_e,L} = 0.997649$ as shown in Table II). In Ref. [44], oblique corrections to the W, Z, and γ propagators, namely, Peskin-Takeuchi S, T, U parameters, [51] due to the KK modes of quarks and leptons, have been evaluated. It has been shown that as a result of the coupling sum rules the oblique corrections are small. The contributions of KK excited modes of quark-lepton multiplets to S, T, and U per KK level are $\delta S \sim 0.002$, $\delta T \sim 0.02$, and $\delta U \sim 10^{-5}$ [44]. Contributions to oblique parameters of $W^{(n)}$, $W_R^{(n)}$ $(n \geq 1)$

also need to be taken into account for complete analysis. We expect that they are small as well. It is reasonable to approximate $\Delta r^{\rm loop}_{\rm GHU}$ by $\Delta r^{\rm loop}_{\rm SM}$. In the evaluation below, we take $\Delta r^{\rm loop}_{\rm GHU} = \Delta r^{\rm loop}_{\rm SM} = 0.0383$.

Now, one can evaluate m_W for given $m_{\rm KK}$ and θ_H. Specify a tentative value for $\sin^2\theta^0_W$, with which one determines m_W from (3.4) and also from (3.6). The two values generally differ from each other. We adjust $\sin^2\theta^0_W$ such that these two values for m_W coincide. In this manner m_W and $\sin^2\theta^0_W$ are determined to satisfy (3.4) and (3.6) simultaneously. For $m_{\rm KK} = 13$ TeV and $\theta_H = 0.10$, for instance, we find that $m_W = 80.396$ GeV, $\sin^2\theta^0_W = 0.22266$, $\hat{g}^{W^{(0)}}_{e\nu_e,L}\hat{g}^{W^{(0)}}_{\mu\nu_\mu,L} = 0.99530$, and $\Delta r_G = 0.0020$.

In Fig. 1 the predicted values for m_W are plotted for various values of $m_{\rm KK}$ and θ_H. It is seen that m_W in GHU becomes larger than $m^{\rm SM}_W$ in the SM, but is smaller than $m^{\rm CDF}_W$ for $13 \le m_{\rm KK} \le 20$ TeV. The GUT inspired GHU in the RS space naturally predicts the W boson mass well above $m^{\rm SM}_W$. We note that an uncertainty Δm_W of about 7 MeV is expected as in the SM for an uncertainty in $m^{\rm SM}_W$.

In Figs. 2–4, $\sin^2\theta^0_W$, $\hat{g}^{W^{(0)}}_{e\nu_e,L}\hat{g}^{W^{(0)}}_{\mu\nu_\mu,L}$ and Δr_G are displayed, respectively. It is observed that these quantities are mostly determined by the value of θ_H. It is seen in Fig. 2 that $\sin^2\theta^0_W$ in the on-shell scheme in GHU approaches $s^2_W|_{\rm SM} = 1 - (m^2_W/m^2_Z)$ in the on-shell scheme in the SM as $m_{\rm KK}$ becomes larger. Similarly, $\hat{g}^{W^{(0)}}_{e\nu_e,L}\hat{g}^{W^{(0)}}_{\mu\nu_\mu,L}$ and Δr_G also approach those in the SM as $m_{\rm KK}$ becomes large.

To compare the result in GHU to that in the SM, let us rewrite the formula (3.6) in the form

$$\frac{G_\mu}{\sqrt{2}} = C\frac{\pi\alpha}{2s^2_{W,\rm GHU}}\frac{1}{m^2_{W^{(0)}}}(1+\Delta r^{\rm loop}_{\rm GHU}),$$
$$C = \frac{s^2_{W,\rm GHU}}{\sin^2\theta^0_W}\hat{g}^{W^{(0)}}_{\mu\nu_\mu,L}\hat{g}^{W^{(0)}}_{e\nu_e,L}(1+\Delta r_G), \qquad (3.9)$$

where $s^2_{W,\rm GHU} = 1 - (m^2_{W^{(0)}}/m^2_Z)$. There are three factors in C. For $m_{\rm KK} = 13$ TeV and $\theta_H = 0.10$ one finds $s^2_{W,\rm GHU}/\sin^2\theta^0_W = 1.00014$, $\hat{g}^{W^{(0)}}_{\mu\nu_\mu,L}\hat{g}^{W^{(0)}}_{e\nu_e,L} = 0.99530$, $1 + \Delta r_G = 1.0020$, and therefore $C = 0.997425 < 1$. In other words, the effective $\Delta r^{\rm eff}_{\rm GHU}$ defined by $1 + \Delta r^{\rm eff}_{\rm GHU} = C(1 + \Delta r^{\rm loop}_{\rm GHU})$ becomes smaller than $\Delta r^{\rm loop}_{\rm GHU} \sim \Delta r^{\rm loop}_{\rm SM}$, which in turn makes $m^{(0)}_W$ larger than $m^{\rm SM}_W$.

In Figs. 1–4 the range of θ_H is restricted to $\theta^{\rm min}_H \le \theta_H \le \theta^{\rm max}_H$, once $m_{\rm KK}$ is specified. For $\theta_H < \theta^{\rm min}_H$, the top quark mass m_t cannot be reproduced. The top quark mass $m_t = k\lambda_t$ is determined by

$$S_L(1;\lambda_t,c_t;z_L)S_R(1;\lambda_t,c_t;z_L) + \sin^2\frac{\theta_H}{2} = 0, \qquad (3.10)$$

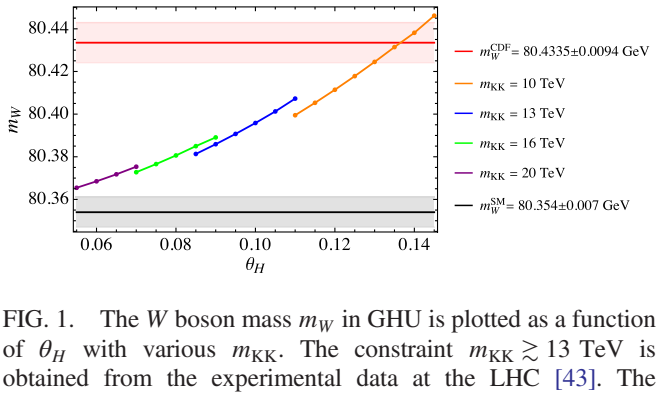

FIG. 1. The W boson mass m_W in GHU is plotted as a function of θ_H with various $m_{\rm KK}$. The constraint $m_{\rm KK} \gtrsim 13$ TeV is obtained from the experimental data at the LHC [43]. The predicted m_W in GHU for $13 \le m_{\rm KK} \le 20$ TeV lies between $m^{\rm SM}_W$ and $m^{\rm CDF}_W$.

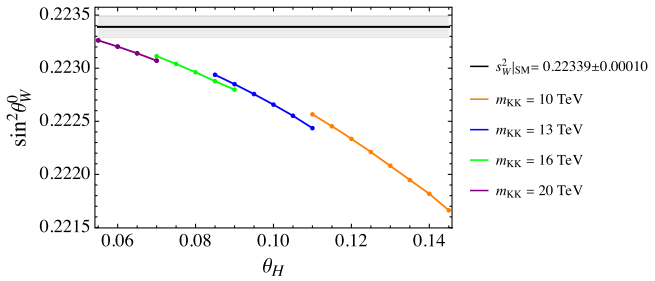

FIG. 2. $\sin^2\theta^0_W$ in the on-shell scheme is plotted as a function of θ_H with various $m_{\rm KK}$. $s^2_W|_{\rm SM} = 1 - (m^2_W/m^2_Z) = 0.22339 \pm 0.00010$ is the value in the on-shell scheme in the SM, listed in Table 10.2 of Ref. [49].

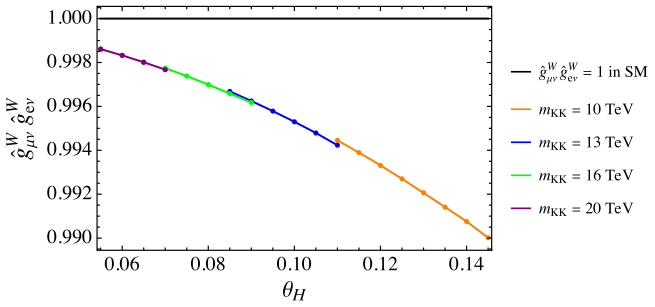

FIG. 3. The product of the W couplings of μ and e normalized by the SM coupling $g_w/\sqrt{2}$, $\hat{g}^W_{\mu\nu}\hat{g}^W_{e\nu} \equiv \hat{g}^{W^{(0)}}_{\mu\nu_\mu,L}\hat{g}^{W^{(0)}}_{e\nu_e,L}$, is plotted as a function of θ_H with various $m_{\rm KK}$.

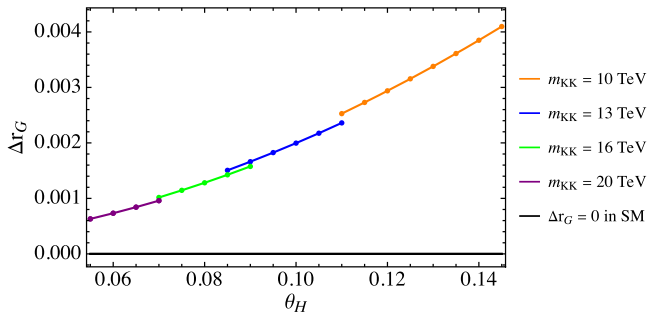

FIG. 4. Δr_G in Eq. (3.6) is plotted as a function of θ_H with various $m_{\rm KK}$. $\Delta r_G = 0$ in the SM.

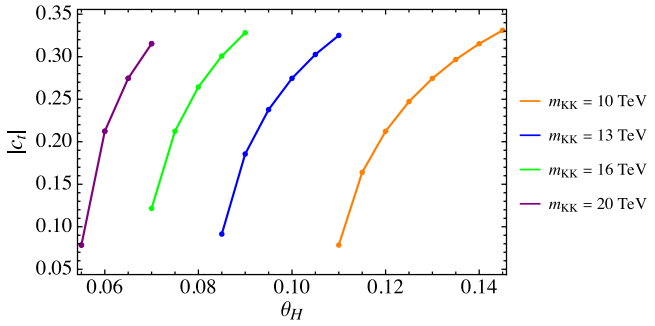

FIG. 5. The absolute value of the bulk mass parameter of the top quark multiplet field c_t is plotted as a function of θ_H with various m_{KK}.

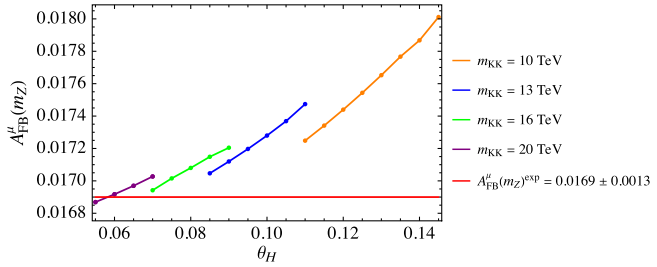

FIG. 7. The forward-backward asymmetry in the process $e^-e^+ \to \mu^-\mu^+$ at the Z pole $A^{\mu}_{FB}(m_Z)$ is plotted as a function of θ_H with various m_{KK}. $A^{\mu}_{FB}(m_Z)$ for $13 \le m_{KK} \le 20$ TeV is consistent with the observed value $A^{\mu}_{FB}(m_Z)^{exp} = 0.0169 \pm 0.0013$.

where c_t is the bulk mass parameter of the top quark field and $S_{L/R}(z;\lambda,c,z_L)$ is given by Eq. (A3). Equation (3.10) is invariant under $c_t \to -c_t$. With given θ_H, z_L, and λ_t, a solution for $|c_t|$ exists only for $\theta_H \ge \theta_H^{min}$ ($c_t = 0$ for $\theta_H = \theta_H^{min}$). In Fig. 5, $|c_t|$ as a function of θ_H with various m_{KK} is displayed. We note that the bulk mass parameters of the other up-type quarks and charged leptons are determined by the same form of the equations as Eq. (3.10). For $m_{KK} = 13$ TeV and $\theta_H = 0.1$, for instance, one finds $(c_u, c_c, c_t) = (-0.863, -0.722, -0.275)$ and $(c_e, c_\mu, c_\tau) = (-1.012, -0.796, -0.677)$. The mass hierarchy of quarks and leptons is naturally explained by $O(1)$ bulk mass parameters in GHU. Only the top quark field has $|c_t| < \frac{1}{2}$ as $m_t > m_W$. In the GUT inspired GHU, negative values for the bulk mass parameters for quark and lepton multiplet fields have been adopted. Positive bulk mass parameters would lead to additional MeV scale neutrinos in the lepton sector and additional very light KK modes of down-type quarks in the first and second generations, the latter of which conflicts with the observation [32].

The value of θ_H is also constrained by $\theta_H < \theta_H^{max}$. It turns out that for $\theta_H > \theta_H^{max}$ the μ-e universality is spoiled, particularly in the Z couplings of the right-handed e and μ at the m_Z scale. For instance, with $m_{KK} = 13$ TeV, the μ-e universality holds within an error of 3×10^{-6} for $0.09 \le \theta_H \le 0.11$, but the universality breaks with a magnitude 3×10^{-3} for $\theta_H = 0.115$. It seems to be related to the fact that the AdS curvature ($\Lambda = -6k^2$) becomes large. $8 \times 10^{12} \le k \le 3 \times 10^{17}$ GeV for $0.09 \le \theta_H \le 0.11$, whereas $k = 6 \times 10^{18}$ GeV for $\theta_H = 0.115$, the value of k getting close to the Planck mass scale. See Fig. 6. We also note that another constraint $m_{KK} \gtrsim 13$ TeV is obtained from the experimental data at the LHC [43].

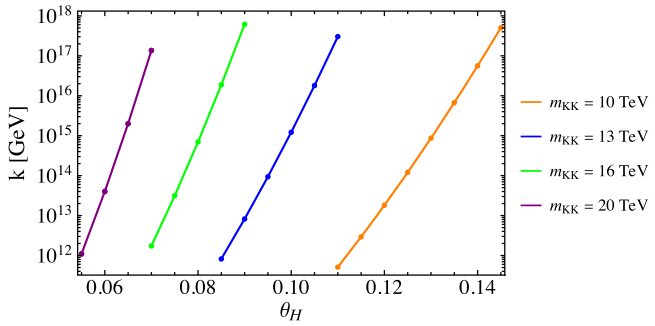

FIG. 6. The parameter k in the AdS curvature of the RS warped space $\Lambda = -6k^2$ is depicted as a function of θ_H with various m_{KK}. As k approaches the Planck mass scale, the μ-e universality starts to break down.

Once m_{KK} and θ_H are specified, $\sin^2\theta_W^0$ in the on-shell scheme in GHU is determined as described above. Now we estimate the forward-backward asymmetry A^{μ}_{FB} in the $e^-e^+ \to \mu^-\mu^+$ process at the m_Z pole. For this end, we need to know $\sin^2\bar{\theta}_W^0(m_Z)$ at the m_Z scale corresponding to $\hat{s}_Z^2 = \sin^2\hat{\theta}_W(m_Z)$ in the $\overline{\rm MS}$ scheme in the SM [49]. In relating $\sin^2\theta_W^0$ to $\sin^2\bar{\theta}_W^0(m_Z)$, only SM particles are relevant, as all KK modes are very heavy ($m_{KK} \gg m_Z$). Further, the couplings among SM particles in GHU are nearly the same as those in the SM. Therefore, it is reasonable to approximate as $\sin^2\bar{\theta}_W^0(m_Z) \sim K_{SM}\sin^2\theta_W^0$, where $K_{SM} = \hat{s}_Z^2/s_W^2 \sim 0.23122/0.22339$ [49]. With this $\sin^2\bar{\theta}_W^0(m_Z)$ one evaluates the Z couplings of e and μ at the m_Z scale, from which $A^{\mu}_{FB}(m_Z)$ is determined. The result is plotted in Fig. 7. It is seen that the predicted values in GHU are consistent with the experimental data $A^{\mu}_{FB}(m_Z)^{exp} = 0.0169 \pm 0.0013$ for $13 \le m_{KK} \le 20$ TeV.

IV. SUMMARY

In this paper, we have evaluated the W boson mass in the GUT inspired GHU in the RS space. With the KK mass scale m_{KK} specified, the allowed range of the AB phase θ_H is constrained as $\theta_H^{min} \le \theta_H \le \theta_H^{max}$. For $m_{KK} = 13$ TeV, for instance, $0.085 \lesssim \theta_H \lesssim 0.11$, and the predicted m_W is $80.381 \lesssim m_W \lesssim 80.407$ GeV. The result for other values of m_{KK} is depicted in Fig. 1. For $13 \le m_{KK} \le 20$ TeV, the predicted m_W lies between the SM value $m_W^{SM} = 80.354 \pm 0.007$ and the CDF value $m_W^{CDF} = 80.4335 \pm 0.0094$ GeV.

In the GUT inspired GHU, the value of m_W is determined by (3.4) and (3.6). In addition to $W = W^{(0)}$, the KK excited modes $W^{(n)}$ and $W_R^{(n)}$ $(n \geq 1)$ mediate the μ decay at the tree level. The W couplings of e and μ, $\hat{g}^{W^{(0)}}_{e\nu_e,L}$ and $\hat{g}^{W^{(0)}}_{\mu\nu_\mu,L}$, become slightly smaller than those in the SM, which leads to a larger value for m_W than that in the SM. It is curious that m_W is mostly determined by the value of the AB phase θ_H as seen in Fig. 1.

It is extremely important to definitively determine m_W by experiments. The W^+W^- production process in the e^+e^- collisions near the threshold should give indispensable information on m_W. Once m_W is determined, the values of $m_{\rm KK}$ and θ_H in GHU can be severely constrained.

ACKNOWLEDGMENTS

This work was supported in part by the Ministry of Science and Technology of Taiwan under Grant No. MOST-111-2811-M-002-047-MY2 (N. Y.).

APPENDIX: BASIS FUNCTIONS

We summarize the basis functions used for wave functions of gauge and fermion fields. For gauge fields, we introduce

$$\begin{aligned}
F_{\alpha,\beta}(u,v) &\equiv J_\alpha(u)Y_\beta(v) - Y_\alpha(u)J_\beta(v),\\
C(z;\lambda,z_L) &= \frac{\pi}{2}\lambda z z_L F_{1,0}(\lambda z,\lambda z_L),\\
S(z;\lambda,z_L) &= -\frac{\pi}{2}\lambda z F_{1,1}(\lambda z,\lambda z_L),\\
C'(z;\lambda,z_L) &= \frac{\pi}{2}\lambda^2 z z_L F_{0,0}(\lambda z,\lambda z_L),\\
S'(z;\lambda,z_L) &= -\frac{\pi}{2}\lambda^2 z F_{0,1}(\lambda z,\lambda z_L),
\end{aligned} \tag{A1}$$

where $J_\alpha(u)$ and $Y_\alpha(u)$ are Bessel functions of the first and second kind. They satisfy

$$-z\frac{d}{dz}\frac{1}{z}\frac{d}{dz}\begin{pmatrix} C \\ S \end{pmatrix} = \lambda^2\begin{pmatrix} C \\ S \end{pmatrix}, \tag{A2}$$

with the boundary conditions $C(z_L;\lambda,z_L) = z_L$, $C'(z_L;\lambda,z_L) = S(z_L;\lambda,z_L) = 0$, $S'(z_L;\lambda,z_L) = \lambda$, and $CS' - SC' = \lambda z$.

For fermion fields with a bulk mass parameter c, we define

$$\begin{aligned}
\begin{pmatrix} C_L \\ S_L \end{pmatrix}(z;\lambda,c,z_L) &= \pm\frac{\pi}{2}\lambda\sqrt{zz_L}F_{c+\frac{1}{2},c\mp\frac{1}{2}}(\lambda z,\lambda z_L),\\
\begin{pmatrix} C_R \\ S_R \end{pmatrix}(z;\lambda,c,z_L) &= \mp\frac{\pi}{2}\lambda\sqrt{zz_L}F_{c-\frac{1}{2},c\pm\frac{1}{2}}(\lambda z,\lambda z_L).
\end{aligned} \tag{A3}$$

These functions satisfy

$$\begin{aligned}
D_+(c)\begin{pmatrix} C_L \\ S_L \end{pmatrix} &= \lambda\begin{pmatrix} S_R \\ C_R \end{pmatrix},\\
D_-(c)\begin{pmatrix} C_R \\ S_R \end{pmatrix} &= \lambda\begin{pmatrix} S_L \\ C_L \end{pmatrix}, \qquad D_\pm(c) = \pm\frac{d}{dz} + \frac{c}{z},
\end{aligned} \tag{A4}$$

with the boundary conditions $C_{R/L} = 1$, $S_{R/L} = 0$ at $z = z_L$, and $C_L C_R - S_L S_R = 1$.

[1] T. Aaltonen *et al.* (CDF Collaboration), High-precision measurement of the W boson mass with the CDF II detector, Science **376**, 170 (2022).

[2] J. Haller, A. Hoecker, R. Kogler, K. Mönig, and J. Stelzer, Status of the global electroweak fit with Gfitter in the light of new precision measurements, Proc. Sci. ICHEP2022 (**2022**) 897.

[3] M. Awramik, M. Czakon, A. Freitas, and G. Weiglein, Precise prediction for the W-boson mass in the standard model, Phys. Rev. D **69**, 053006 (2004); arXiv:hep-ph/0311148v3.

[4] J. de Blas, M. Pierini, L. Reina, and L. Silvestrini, Impact of the recent measurements of the top-quark and W-boson masses on electroweak precision fits, Phys. Rev. Lett. **129**, 271801 (2022).

[5] The ATLAS Collaboration, Improved W boson mass measurement using $\sqrt{s} = 7$ TeV proton-proton collisions with the ATLAS detector, Report No. ATLAS-CONF-2023-004, https://cds.cern.ch/record/2853290/files/ATLAS-CONF-2023-004.pdf.

[6] C-T. Lu, L. Wu, Y. Wu, and B. Zhu, Electroweak precision fit and new physics in light of the W boson mass, Phys. Rev. D **106**, 035034 (2022).

[7] A. Strumia, Interpreting electroweak precision data including the W-mass CDF anomaly, J. High Energy Phys. 08 (2022) 248.

[8] G. Cacciapaglia and F. Sannino, The W boson mass weighs in on the non-standard Higgs, Phys. Lett. B **832**, 137232 (2022).

[9] E. Bagnaschi, J. Ellis, M. Madigan, K. Mimasu, V. Sanze, and T. You, SMEFT analysis of m_W, J. High Energy Phys. 08 (2022) 308.

[10] P. Asadi, C. Cesarotti, K. Fraser, S. Homiller, and A. Parikh, Oblique lessons from the W-mass measurement at CDF II, Phys. Rev. D **108**, 055026 (2023).

[11] K. S. Babu, S. Jana, and Vishnu P. K., Correlating W-boson mass shift with muon $g-2$ in the two Higgs doublet model, Phys. Rev. Lett. **129**, 121803 (2022).

[12] S. Kanemura and K. Yagyu, Implication of the W boson mass anomaly at CDF II in the Higgs triplet model with a mass difference, Phys. Lett. B **831**, 137217 (2022).

[13] H. M. Lee and K. Yamashita, A model of vector-like leptons for the muon $g-2$ and the W boson mass, Eur. Phys. J. C **82**, 661 (2022).

[14] J. Kawamura, S. Okawa, and Y. Omura, W boson mass and muon $g-2$ in a lepton portal dark matter model, Phys. Rev. D **106**, 015005 (2022).

[15] K. I. Nagao, T. Nomura, and H. Okada, A model explaining the new CDF II W boson mass linking to muon $g-2$ and dark matter, Eur. Phys. J. Plus **138**, 365 (2023).

[16] M. Endo and S. Mishima, New physics interpretation of W-boson mass anomaly, Phys. Rev. D **106**, 115005 (2022).

[17] M. Blennow, P. Coloma, E. Fernandez-Martinez, and M. Gonzalez-Lopez, Right-handed neutrinos and the CDF II anomaly, Phys. Rev. D **106**, 073005 (2022).

[18] Y. Hosotani, Dynamical mass generation by compact extra dimensions, Phys. Lett. **126B**, 309 (1983).

[19] A. T. Davies and A. McLachlan, Gauge group breaking by Wilson loops, Phys. Lett. B **200**, 305 (1988).

[20] Y. Hosotani, Dynamics of nonintegrable phases and gauge symmetry breaking, Ann. Phys. (N.Y.) **190**, 233 (1989).

[21] A. T. Davies and A. McLachlan, Congruency class effects in the Hosotani model, Nucl. Phys. **B317**, 237 (1989).

[22] H. Hatanaka, T. Inami, and C. S. Lim, The gauge hierarchy problem and higher dimensional gauge theories, Mod. Phys. Lett. A **13**, 2601 (1998).

[23] H. Hatanaka, Matter representations and gauge symmetry breaking via compactified space, Prog. Theor. Phys. **102**, 407 (1999).

[24] M. Kubo, C. S. Lim, and H. Yamashita, The Hosotani mechanism in bulk gauge theories with an orbifold extra space S^1/Z_2, Mod. Phys. Lett. A **17**, 2249 (2002).

[25] C. A. Scrucca, M. Serone, and L. Silvestrini, Electroweak symmetry breaking and fermion masses from extra dimensions, Nucl. Phys. **B669**, 128 (2003).

[26] K. Agashe, R. Contino, and A. Pomarol, The minimal composite Higgs model, Nucl. Phys. **B719**, 165 (2005).

[27] G. Cacciapaglia, C. Csaki, and S. C. Park, Fully radiative electroweak symmetry breaking, J. High Energy Phys. 03 (2006) 099.

[28] A. D. Medina, N. R. Shah, and C. E. M. Wagner, Gauge-Higgs unification and radiative electroweak symmetry breaking in warped extra dimensions, Phys. Rev. D **76**, 095010 (2007).

[29] Y. Hosotani, K. Oda, T. Ohnuma, and Y. Sakamura, Dynamical electroweak symmetry breaking in $SO(5)\times U(1)$ gauge-Higgs unification with top and bottom quarks, Phys. Rev. D **78**, 096002 (2008); **79**, 079902(E) (2009).

[30] S. Funatsu, H. Hatanaka, Y. Hosotani, Y. Orikasa, and T. Shimotani, Novel universality and Higgs decay $H\to\gamma\gamma, gg$ in the $SO(5)\times U(1)$ gauge-Higgs unification, Phys. Lett. B **722**, 94 (2013).

[31] J. Yoon and M. E. Peskin, Dissection of an $SO(5)\times U(1)$ gauge-Higgs unification model, Phys. Rev. D **100**, 015001 (2019).

[32] S. Funatsu, H. Hatanaka, Y. Hosotani, Y. Orikasa, and N. Yamatsu, GUT inspired $SO(5)\times U(1)\times SU(3)$ gauge-Higgs unification, Phys. Rev. D **99**, 095010 (2019).

[33] S. Funatsu, H. Hatanaka, Y. Hosotani, Y. Orikasa, and N. Yamatsu, CKM matrix and FCNC suppression in $SO(5)\times U(1)\times SU(3)$ gauge-Higgs unification, Phys. Rev. D **101**, 055016 (2020).

[34] S. Funatsu, H. Hatanaka, Y. Hosotani, Y. Orikasa, and N. Yamatsu, Effective potential and universality in GUT-inspired gauge-Higgs unification, Phys. Rev. D **102**, 015005 (2020).

[35] Y. Hosotani and N. Yamatsu, Gauge-Higgs grand unification, Prog. Theor. Exp. Phys. **2015**, 111B01 (2015); A. Furui, Y. Hosotani, and N. Yamatsu, Toward realistic gauge-Higgs grand unification, Prog. Theor. Exp. Phys. **2016**, 093B01 (2016).

[36] S. Funatsu, H. Hatanaka, Y. Hosotani, and Y. Orikasa, Distinct signals of the gauge-Higgs unification in e^+e^- collider experiments, Phys. Lett. B **775**, 297 (2017).

[37] J. Yoon and M. E. Peskin, Fermion pair production in $SO(5)\times U(1)$ gauge-Higgs unification models, arXiv:1811.07877.

[38] S. Funatsu, Forward-backward asymmetry in the gauge-Higgs unification at the international linear collider, Eur. Phys. J. C **79**, 854 (2019).

[39] S. Funatsu, H. Hatanaka, Y. Hosotani, Y. Orikasa, and N. Yamatsu, Fermion pair production at e^-e^+ linear collider experiments in GUT inspired gauge-Higgs unification, Phys. Rev. D **102**, 015029 (2020).

[40] S. Funatsu, H. Hatanaka, Y. Hosotani, Y. Orikasa, and N. Yamatsu, Bhabha scattering in the gauge-Higgs unification, Phys. Rev. D **106**, 015010 (2022).

[41] S. Funatsu, H. Hatanaka, Y. Orikasa, and N. Yamatsu, Single Higgs boson production at electron-positron colliders in gauge-Higgs unification, Phys. Rev. D **107**, 075030 (2023).

[42] N. Yamatsu, S. Funatsu, H. Hatanaka, Y. Hosotani, and Y. Orikasa, W and Z boson pair production at electron-positron colliders in gauge-Higgs unification, Phys. Rev. D **108**, 115014 (2023).

[43] S. Funatsu, H. Hatanaka, Y. Hosotani, Y. Orikasa, and N. Yamatsu, Signals of W' and Z' bosons at the LHC in the $SU(3)\times SO(5)\times U(1)$ gauge-Higgs unification, Phys. Rev. D **105**, 055015 (2022).

[44] Y. Hosotani, S. Funatsu, H. Hatanaka, Y. Orikasa, and N. Yamatsu, Coupling sum rules and oblique corrections in gauge-Higgs unification, Prog. Theor. Exp. Phys. **2023**, 063B01 (2023).

[45] S. Funatsu, H. Hatanaka, Y. Hosotani, Y. Orikasa, and N. Yamatsu, Anomaly flow by an Aharonov-Bohm phase, Prog. Theor. Exp. Phys. **2022**, 043B04 (2022).

[46] Y. Hosotani, Universality in anomaly flow, Prog. Theor. Exp. Phys. **2022**, 073B01 (2022).

[47] L. Randall and R. Sundrum, A large mass hierarchy from a small extra dimension, Phys. Rev. Lett. **83**, 3370 (1999).

[48] A. Sirlin, Radiative corrections in the $SU(2)_L \times U(1)$ theory: A simple renormalization framework, Phys. Rev. D **22**, 971 (1980).

[49] R. L. Workman *et al.* (Particle Data Group), Reviews, tables & plots, Prog. Theor. Exp. Phys. **2022**, 083C01 (2022).

[50] S. Funatsu, H. Hatanaka, Y. Hosotani, Y. Orikasa, and N. Yamatsu, Electroweak and left-right phase transitions in $SO(5) \times U(1) \times SU(3)$ gauge-Higgs unification, Phys. Rev. D **104**, 115018 (2021).

[51] M. E. Peskin and T. Takeuchi, New constraint on a strongly interacting Higgs sector, Phys. Rev. Lett. **65**, 964 (1990); Estimation of oblique electroweak corrections, Phys. Rev. D **46**, 381 (1992).